Performance and stability of a dynamically controlled EBPR anaerobic/aerobic granular sludge reactor

Performance and Stability of a Dynamically controlled EBPR Anaerobic/Aerobic Granular Sludge Reactor.

Short title: EBPR Anaerobic/aerobic AGS system with an anaerobic and aerobic dynamically controlled step

Flinn De Vleeschauwer[1], Michel Caluwé[1], Thomas Dobbeleers[1], Hannah Stes[1,2], Lennert Dockx[1], Filip Kiekens[3], Jolien D'aes[1],Cosmin Copot[3], Jan Dries[1]

[1]*Research group BioGEM, Bio-Chemical Green Engineering & Materials, Faculty of Applied Engineering, University of Antwerp, Salesianenlaan 90, 2660 Antwerp, Belgium.*

[2]*Pantarein Water BVBA, Egide Walschaersstraat 22L, 2800 Mechelen, Belgium.*

[3]*Laboratory of Pharmaceutical Technology and Biopharmacy, Department of Pharmaceutical Science, University of Antwerp, Universiteitsplein 1, 2610 Wilrijk, Belgium.*

*corresponding author: Jan Dries

Full postal address: University of Antwerp, Salesianenlaan 90, 2660 Antwerp, Belgium. e-mail: jan.dries2@uantwerpen.be; phone number: +32(0)32658872; fax-number: not available.

Abstract

Treatment of rapidly varying wastewaters in anaerobic/aerobic aerobic granular sludge (AGS) systems remains problematic. This study investigated AGS formation and the impact of varying COD and phosphorus concentrations on an enhanced biological phosphorus removal (EBPR) AGS SBR with a conductivity based anaerobic and OUR based aerobic dynamically controlled step. Phase 1 investigated the development of AGS. Phase 2 examined the flexibility of the dynamic control strategy and AGS efficiency while rapidly altering the influent composition. AGS was formed successfully in phase 1: the DV50 increased to 285 µm., and the SVI5 and SVI30 decreased to 51 and 40 ml/g respectively. In phase 2 the effluent COD and PO4-P concentration remained low at respectively 58 ± 27 mg/L and 0.53 ± 0.77 mg/L. With an anaerobic DOC uptake efficiency of 98.4 ± 0.9 %.

Keywords: Anaerobic dynamic control strategy; synthetic wastewater; phosphate accumulating organisms (PAO)

1.0 Introduction

In the past 2 decades, the aerobic granular sludge (AGS) technology has shown to have high potential in the treatment of wastewater. A total of 42 full-scale sewage wastewater treatment plants and 6 full scale industrial wastewater treatment plants have been reported worldwide (website Nereda). The large difference between the number of domestic and industrial full-scale AGS wastewater treatment plants can be explained by the difficulty of treating complex and variable wastewater such as industrial wastewater. A possible AGS operational method for the treatment of industrial wastewater is a anaerobic/aerobic AGS sequencing batch reactor (SBR) with a low hydraulic selection pressure. An anaerobic/aerobic operation stimulates the growth of granules with slow growing polyphosphate accumulating and glycogen accumulating organisms (PAO and GAO) (de Kreuk et al 2004). This kind of AGS SBRs requires a complete COD uptake during the anaerobic step by PAO and GAOs. A weakness to this kind of systems is floccular sludge formation due to “aerobic COD leakage” resulting from an incomplete COD uptake in the anaerobic step. As such, aerobic COD leakage feeds the aerobic floccular sludge (de Pronk et al. 2015). With a static anaerobic step in the treatment process, the risk of aerobic COD leakage increases when using varying COD concentrations due to a possible incomplete COD uptake in the anaerobic step.

An innovative solution is the use of sensor guided dynamically controlled anaerobic/aerobic AGS systems. Such AGS systems would automatically

elongate or shorten anaerobic and/or aerobic steps to ensure an optimal anaerobic and aerobic efficiency, hereby reducing aerobic COD leakage and improving the AGS formation.

Extensive research in static controlled anaerobic/aerobic AGS systems has been carried out (e.g. De Kreuk et al. 2004). In contrast, only a few reports on dynamically controlled anaerobic/aerobic AGS systems have been published: In a simultaneous nitrification denitrification (SND) anaerobic/aerobic AGS system treating potato industrial wastewater, the oxygen uptake rate (OUR) and the pH profile have been used successfully to control the duration of the aerobic step (Dobbeleers et al. 2017). Stes et al. (2018) have reported a successful implementation of an OUR based strategy in an anaerobic/aerobic AGS system treating brewery wastewater.

In an EBPR system the conductivity profile can be used to control the anaerobic step. The change in conductivity is well correlated with the change in the anaerobic PO_4-P release rate because of the additional release of potassium and magnesium ions during the anaerobic PO_4-P release. (Maurer et al. 1995). Kishida et al. (2008) have used the anaerobic conductivity profile and aerobic pH profile to dynamically control the anaerobic and aerobic steps in an EBPR AGS system, resulting in stable nitrogen and phosphorus removal even during 8 days of influent variations. Long term studies on AGS systems with changing influent compositions and a conductivity based anaerobic dynamically controlled step have not yet been reported.

The current study investigates the performance of an EBPR AGS SBR using a conductivity based anaerobic dynamic control strategy and an OUR

based aerobic dynamic control strategy. The study was carried out in two phases. Phase 1 focuses on the formation and performance of an EBPR AGS SBR while applying an anaerobic and aerobic dynamic control strategy and feeding the reactor with an influent with a constant composition. Phase 2 investigates the prolonged effect on the EBPR AGS system efficiency and the impact on the anaerobic and aerobic dynamic control strategy while feeding the reactor an influent with rapidly varying compositions.

2.0 Material and methods

2.1 Reactor set-up and operation

The study was carried out in two phases. Phase 1 (reactor A) investigated AGS formation in an anaerobic/aerobic dynamically controlled EBPR AGS SBR. Phase 2 (reactors B and C) examined the flexibility of the dynamic control strategy and the AGS efficiency when feeding influent with rapidly varying compositions. Reactor C was the control reactor which was fed a constant influent composition.

In the first phase the reactor had a working volume of 11.1L. For the second phase both reactors had a working volume of 6L. The reactors were equipped with an influent peristaltic pump (Watson Marlow®), a mixer (Heidolph® RZR2020), a discharge valve (Eriks RX ER10.X33.S00) and an aeration system consisting of an aeration pump (koi flow 60, Aquadistri China®) and a 13 cm aeration disc (Aquadistri China®). Furthermore the reactors were equipped with a luminescent dissolved oxygen (LDO) sensor (Hang Lange®), a pH sensor (JUMO® BlackLine) and a 3798-S digital inductive conductivity

sensor (Hach Lange®). All sensor values were logged. At the end of each cycle the values were archived.

The SBRs were operated with a custom built National Instruments LabVIEW® program, a Siemens PLC and a Phoenix IO. The reactor cycles had 9 steps; idle step (10 seconds); aerated pre-step (30 minutes); unaerated step (10 minutes); anaerobic influent feeding step (flow dependent); anaerobic step (dynamic); aerobic step (dynamic); sludge settling step (10 minutes); discharge step (5 minutes); inactive step (1 minute). The duration of the feeding step varied between 1 and 2 minutes.

Reactor A was seeded with 10.1L sludge from a local EBPR activated sludge municipal wastewater treatment plant (Aquafin Antwerpen Zuid). The seed sludge MLSS, MLVSS, SVI30 and DV50 values were respectively 3.712 ±0.011 g/L, 2.682 ±0.216 g/L, 76 ml/g and 128 ±2.16 µm. Reactor B and C were seeded with sludge from reactor A.

During phase 1 reactor A was fed 1L influent per cycle, had a working volume of 11.1L and a volume exchange rate (VER) of about 9%. The VER of reactor B and C in phase 2 was approximately 8% with a influent feed of 0.48 L and a working volume of 6L. The sludge retention time (SRT) was kept at 30 days throughout the study. The hydraulic retention time (HRT) and organic loading rate (OLR) varied due to the dynamic cycle durations and the varying influent composition in phase 2.

2.2 Influent composition

The reactors were fed with synthetic wastewater. The influent composition of reactor A and C was kept constant (Influent 1): 1250 mgCOD/L (Na-

propionate), 25 mgPO_4-P/L (K_2HPO_4), 25 mgNH_4-N/L (NH_4Cl), 75 mgCO_3^{2-}/L ($NaHCO_3^{2-}$), 26 mgMg/L ($MgSO_4x6H_20$), 56 mgK^{1+}/L (KCl) and 1ml/L trace solution (Vishniac and Santer 1957). To inhibit nitrification, N-allylthiourea (ATU) was added to the influent at 10 mg/L.

The influent composition of reactor B was varied. The impact of three influent variation strategies (IVS) was investigated. 1) IVS_1 (day 8 to day 62): The COD and PO_4-P concentrations were varied step by step, first with small COD and PO_4-P variations (± 15% compared to influent 1, COD concentration between 1156 and 1437 mg/L) followed by increasing variations(up to ± 40% compared to influent 1, COD concentration between 750 and 1750 mg/L). Meanwhile the COD/P ratio was kept constant at 50. 2) IVS_2 (day 63 to day 99): the PO_4-P concentration was varied step by step (± 60% compared to influent 1, PO_4-P concentration between 10 and 40 mg/L) while the COD concentration was kept constant at 1250 mg/L with Na-propionate. 3) IVS_3 (day 100 to day 115): The influent composition strategies of IVS_1 and IVS_2 were combined. The COD/P ratio was varied (between 21 and 116) by changing both the COD and PO_4-P concentrations step by step (± 40% compared to influent 1). The ATU and CO_3^{2-} concentrations and the COD/N/K/Mg ratios were kept constant.

2.3 Dynamic control strategy

The anaerobic and aerobic dynamically controlled systems both worked as closed-loop control systems. Sensor profile patterns determined the duration of the anaerobic and aerobic step.

The aerobic step was dynamically controlled by means of the oxygen uptake rate (OUR). The OUR calculation and the aerobic dynamic control strategy were used as described in Dobbeleers et al. (2017). The oxygen level in the reactors were controlled with an on/off aeration control, keeping the oxygen concentration between 1 and 2 mg/L. This resulted in an oxygen profile with alternating positive and negative flanks. A custom built LabVIEW program calculated the OUR (mgO2/L.h) during the negative flanks. The aerobic dynamic control strategy used two set point, SP_{OUR1} and SP_{OUR2}. When a fixed number (SP_{OUR1}) of consecutive OUR values dropped below a minimal set point (SP_{OUR2}), the aerobic step was terminated. The SP_{OUR1} and SP_{OUR2} were periodically adjusted to ensure a complete PO_4-P uptake. SP_{OUR2} was adjusted to ensure that the specific respiration speed (SOUR) decreased to 2.5 mg/g_{MLVSS}.h. SP_{OUR2} was increased or decreased to guarantee that the effluent PO_4-P was below 1 mg/L. To rule out premature or overdue terminations of the aerobic step, the aerobic dynamic control strategy had a built-in minimal and maximal duration of respectively 1and 5 hours. The aeration step in reactor A, B and C were operated with the same aerobic dynamic control strategy.

As described by Kishida et al. (2008), the duration of the anaerobic step in an EBPR AGS SBR can be controlled by the conductivity slope (µS/m.d). The change in conductivity is well correlated to the PO_4-P concentration. The additional release of magnesium and potassium ions during the phosphate release contributes to the increase in the conductivity (Maurer et al. 1995). When the anaerobic phosphate release terminates, the conductivity slope becomes equal to zero, hereby giving a good indication of the PO_4-P concentration profile.

The anaerobic dynamic control system calculates the moving conductivity slope (MCS) during the anaerobic step. The control strategy uses 4 calculation variables (CV); the intervals of the sensor value (CV_1) and the number of sensor values per MCS calculation (CV_2). The cut-off point is determined by a minimal MCS (CV_3) and the number of MCS's (CV_4) that meet the cut-off requirements. In total the anaerobic dynamic control strategy ran through 3 loops to dynamically control the duration of the anaerobic step (Figure 1).

To obtain an accurate and stable anaerobic step termination the optimal CVs set points were tested by looking at the conductivity, pH, DOC uptake and PO_4-P release profiles of an AGS SBR. The use of higher CV_1 and CV_2 values resulted in smooth MCS profiles (high stability) but caused a longer delay on the cut-off point (low accuracy). A CV_1 value of 60 seconds and a CV_2 value of 10 resulted in the stable MCS profile with an acceptable delay (±10 minutes delay). During phase 1 the CV_3 value was adjusted depending on the evolution of the DOC uptake and PO_4-P release profiles. The CV_4 value was kept constant at 20. The CV_3 and CV_4 values remained unchanged in phase 2. To rule out premature or overdue terminations of the anaerobic step, the anaerobic dynamic control strategy had a built-in minimal and maximal duration of respectively 20 and 120 minutes. The calculated MCS values were logged and archived at the end of each cycle.

2.4 Analytical Methodology

The chemical analyses (total and soluble chemical oxygen demand (COD, sCOD), phosphorus-orthophosphate (PO_4-P), and nitrogen-ammonium (NH_4-N) were analysed with test kits from Hanna Instruments Belgium respectively

HI93754A-25, HI93754B-25, HI93706-01 and HI93715-01. The potassium (K^{1+}) and Magnesium (Mg^{2+}) concentrations were analysed with Hach Lange® test kits, respectively LCK 328 and LCK 326. The dissolved organic carbon (DOC) was analysed with a Sievers InnovOx® laboratory total organic carbon analyser. All parameters except the COD were measured on pre-filtered samples (VWR® glass microfibers filter, 693, particle retention: 1.2µm).

The sludge mixed liquor suspended (volatile) solids (ML(V)SS) and the sludge volume index (SVI) were measured according to the standard methods (APHA, 1998). Microscopic images were taken with a MOTIC BA310 microscope (Opti-service, Belgium).

The sludge particle size distribution (DV50) was measured with a Malvern Mastersizer 3000 as described by Caluwé et al. (2017). To study the evolution of the particle size classes (>200µm), the volume fraction larger than 200 µm ($VF_{>200\mu m}$) was calculated.

Reactor C was operated as a control reactor, only the sludge particle size distribution (DV50) was analysed.

2.5 In-situ cycle measurement

To test the effectiveness of the anaerobic dynamic control strategy, the DOC uptake efficiency and the PO_4-P release efficiency were measured at different moments during the cycle. During the anaerobic step 3 grab samples were taken (Figure 2): at sample point a (SPa) the start of the anaerobic step; at sample point b (SPb), during the anaerobic step (conductivity profile dependent, when the conductivity slope changed from positive to negative); at sample point c (SPc), at the end of the anaerobic step. During the aerobic step in phase 1, a

sample was taken every hour and at the end of the aerobic step. The aerobic sample frequency was altered in phase 2 to study the relationship between the conductivity profile and the phosphate concentration. Two samples were taken during the aerobic step: one at sample point d (SPd) (conductivity profile dependent, when the conductivity slope changed from negative to positive) and one at sample point e (SPe) at the end of the aerobic step (Figure 2). The DOC and PO_4-P concentrations were measured. The anaerobic DOC uptake efficiency and the anaerobic PO_4-P release efficiency were calculated with following formulas:

$$Anaerobic\ DOC\ uptake\ (\%)\ at\ (b) = 100x\frac{DOC_{(a)} - DOC_{(b)}}{DOC_{(a)} - DOC_{(e)}}$$

$$Total\ anaerobic\ DOC\ uptake\ (\%)\ at\ (c) = 100x\frac{DOC_{(a)} - DOC_{(c)}}{DOC_{(a)} - DOC_{(e)}}$$

$$Anaerobic\ PO_4(P)\ release\ (\%)\ at\ (b) = 100x\frac{PO_4(P)_{(b)} - PO_4(P)_{(a)}}{PO_4(P)_{(c)} - PO_4(P)_{(a)}}$$

With (a) 30 seconds after influent feed, (b) at the sample points (conductivity profile dependent), (c) at the end of the anaerobic step and (e) at the end of the aerobic step (Figure 2). To take into account immediately adsorbed DOC, the DOC concentration at SPa was theoretically calculated using the influent DOC, the effluent DOC and VER.

2.6 DNA extraction

For molecular PAO and GAO community quantification and gene sequencing analysis, 250 µl AGS samples were taken from the reactor

periodically and preserved at -80°C. The DNA was extracted according to the method described in Mcilroy et al. (2008) and stored at -80°C.

2.7 qPCR molecular quantification

A PAO541f/PAO846r primer and a GAOQ989f/GAM1278r primer were used to target respectively PAO (16S rRNA Candidatus Accumulibacter phosphatis) and GAO (16S rRNA Candidatus Competibacter phosphatis) organisms. Universal 1055f/Universal 1392r primers were used to measure the total amount of bacterial DNA (16S rRNA Universal bacteria). The amount of target cells per gMLVSS were calculated from de measured DNA concentrations. The DNA concentrations were quantified according to the method described in Caluwé et al. (2017).

2.8 Microbial community composition

The microbial community composition was obtained by 16S rRNA gene amplification. Barcode primers (IDT) and Phusion High-Fidelity DNA polymerase (Thermo Scientific) were used to generate amplicons targeting the V 1-3 region of the 16S rRNA gene as described by Kozich et al. (2013). The purification of the PCR products was carried out with the SequalPrep Normalization plate kit (Invitrogen) before being pooled. Afterwards NucleoSpin Gel and PCR Clean-up (Macherey Nagel) was used to obtain an enhanced purified library. Before amplicon sequencing, the library was diluted resulting in a 2 nM library. At last the amplicon sequencing was executed on an Illumina Miseq system at the Centre for Medical Genetics (Edegem, Belgium) with the MiSeq Reagent Kit v2 (Illumina). The UPARSE pipeline (Edgar et al. 2013) was used to process the paired-end reads. The results were compared, for

taxonomy predictions of the operational taxonomic unit (OTU) sequences, to a reference database; MiDAS (version 2.1). A name is proposed for all the abundant genus-level taxa present in activated sludge, anaerobic digesters and influent wastewater. The reference database is a manually curated SILVA 16S rRNA taxonomy library (release 1.23 Ref NR99) (McIlroy et al. 2015).

3.0 Results and Discussion

3.1 Phase 1

During phase 1 the formation of granules in an EBPR AGS SBR with dynamically controlled anaerobic and aerobic steps was investigated for 105 days. The duration of the anaerobic step was controlled using the conductivity MCS. The duration of the aerobic step was controlled using the OUR. AGS was formed successfully during phase 1 with an anaerobic and aerobic dynamic control strategy.

3.1.1 Reactor operation and removal efficiency

The first three days the anaerobic step was controlled statically with a fixed duration of 2 hours. From the fourth day onward the anaerobic dynamic control strategy was applied. The anaerobic dynamic set points CV_1, CV_2 and CV_4 were kept respectively at 60(sec), 10 (#) and 20 (#). To optimize the anaerobic step, the cut-off point (CV_3) was systematically increased depending on the stabilization of the conductivity profile.

The reliability, or degree of success, of the anaerobic and aerobic dynamic control strategy was 82.4 %. The control detected the endpoint of the anaerobic

step and terminated the step accordingly. Two factors had a negative effect on the reliability. First, the sporadic activation of the minimal and maximal anaerobic and aerobic step durations occurred due to ineffective filling steps resulting from detached influent tubing. Secondly, a continuous aeration from day 34 to 35 due to an aeration pump malfunction resulted in the loss of the anaerobic PAO conductivity profile. In-situ PO_4-P analysis showed no anaerobic PO_4-P release. A possible cause could be the loss of the microbial stored poly-PO_4-P due to aerobic release and sequential wash-out of the PO_4-P in the effluent. The anaerobic step was operated statically (1.25 h) from day 36-42. On day 43 the anaerobic PAO conductivity profile was re-established and the anaerobic dynamic control strategy was reactivated.

The anaerobic conductivity increase is strongly correlated to the PO_4-P release (Maurer et al. 1995). Therefore the evolution of the MCS profile is a good representation of the evolution of the PAO activity. During the first 56 days, the maximal MCS values did not evolve, stabilizing at 1.55 ± 0.14 µS/cm.d. As time progressed the maximal MCS values increased to 4.04 ± 0.36 µS/cm.day (day 91-110). The increase in the conductivity MCS indicates an increased phosphate release rate. Furthermore the anaerobic step duration is by design strongly correlated to the conductivity MCS profile. While the maximal MCS values remained stable during the first ± 56 days, the anaerobic step duration continually decreased, starting at 1.680 ± 0.23 hours (day 1-7) and systematically decreasing over a period of 73 days to 0.790 ± 0.076 hours (day 68-73). The anaerobic step varied more during first 50 days, these variations are possible caused by an increasing sludge activity as the sludge

concentration increased and the sludge metabolism adapted to the influent composition and reactor operation strategy.

From day 65 to 110 the reactor showed a stabilized operation, the duration of the anaerobic step and the starting MCS value were respectively 0.737 ± 0.069 hour and 3.42 ± 0.59 µS/cm.day.

The sludge PAO activity during stable operation was confirmed through in-situ measurements. The DOC uptake efficiency at SPc and SPd (Figure 2) were respectively 96.9 ± 1.8 % and 97.8 ± 1.4 %. The anaerobic PO_4-P release efficiency at SPc was 94.4 ± 0.3 %.

As reported by Sato et al. (1992), Pijuan et al. (2005) and Oehmen et al. (2005) the anaerobic P release/COD uptake ratio (Pmol/Cmol) of an EBPR system varies between 0.30 to 0.45 Pmol/Cmol. During phase 1 the anaerobic P release/COD uptake ratio during the stable operation was 0.24 ± 0.04 Pmol/Cmol. This is lower than reported values. Oehmen et al. (2006) suggested that lower anaerobic P release/COD uptake ratios could indicate a possible GAO competition for the available substrate during the anaerobic step.

From day 1 to day 110 the aerobic step was dynamically controlled by means of the OUR. SP_{OUR2} was set at 10 mgO_2/L.h. This was reduced to 8 mgO_2/L.h after the first 7 days to improve the PO_4-P uptake efficiently. SP_{OUR2} was kept at 3 for the entire phase 1. The aerobic step took on average 3.09 ± 0.54 h. The OUR profile was strongly correlated to the PO_4-P concentration with R^2 of 0.9992 and a p-value of < 0.0008 (Alfa = 0.05).

During the aeration, the aerobic conductivity profile initially decreased but at a later stage increased again (Figure 3 (a)). In-situ measurements of

magnesium (Mg^{2+}) and potassium (K^{1+}) show a decrease of Mg^{2+} and K^{1+} concentrations during the conductivity decrease. However the K^{1+} concentration increased again at the end of the aerobic step. This indicates that the increase in K^{1+} is potentially the reason for the aerobic conductivity increase.

The anaerobic OLR increased as the sludge PAO activity increased, starting at 1.726 ± 0.225 kgCOD/m³.d and from day 70 to 110 stabilizing at 3.839 ± 0.148 (Figure 3 (d)). This had little effect on the total OLR, which remained stable throughout phase 1 at 0.620 ±0.077 kgCOD/m³.d.

The COD removal efficiency was 97.5 ± 1.1%. No change in the COD efficiency was observed. The aeration pump malfunction between day 33-35 had no effect on the COD removal efficiency, while the impact on the PO_4-P removal efficiency was significant, decreasing from 90.6 ± 5.9% to 81.2 ± 2.9%. The removal efficiency increased again to 90.7 ± 8.5% between day 65-110.

3.1.2 Aerobic Granular Sludge formation and qPCR analysis

The application of an EBPR operation and an anaerobic and aerobic dynamic control strategy resulted in the formation of AGS. On the basis of the MLSS, MLVSS, the particle size distribution (Figure 3 (c)) and microscopic images the sludge morphology experienced three distinct stages (stage 1, 2 and 3): a start-up stage, an AGS germination stage and an AGS maturation stage.

During the first 20 days (stage 1) the MLSS and MLVSS decreased due to the adaptation of the sludge to an EBPR SBR operation and the implementation of a sludge retention time of 30 days. The DV50 increased and the $VF_{>200\mu m}$

increased from 20,0 % to 40,6 %. Microscopic images show a decrease of small sludge particles.

Between day 20 and 57 (stage 2) the MLSS and MLVSS increased and the DV50 stabilized. The $VF_{>200\mu m}$ stabilized at 37,7 ±3,1%. Microscopic images show the reappearance of small sludge agglomerates, indicating the potential growth of small granule-like structures.

From day 57 until day 110 (stage 3) the MLSS and MLVSS stabilized. The DV50 and the $VF_{>200\mu m}$ increased continually, from respectively 153 µm to 285 µm and 40.1 % to 60.2%. The granules increased in size during this stage without an increase in MLSS indicating the development of AGS.

Additionally qPCR and microbial community composition analysis showed an increase in *Candidatus Accumulibacter phosphatis* a PAO (Figure 4). The abundance of *Candidatus Competibacter phosphatis* (a GAO) remained low; 0.58 ±1.06 %. This indicates that the combination of the applied influent COD/P ratio (approximately 50) and an anaerobic/aerobic operational strategy was successful in selecting PAOs over GAOs. Weissbrodt et al. (2013) reported a similar OTU value of 25 % while feeding propionate based wastewater in an anaerobic fed anaerobic/aerobic AGS SBR.

3.2 Phase Two

3.2.1 Reactor operation and removal efficiency

During phase 2 the impact of rapidly varying influent concentrations on the efficiency of the anaerobic and aerobic dynamic control strategy and ASG efficiencies were investigated. The sludge from reactor A was divided in reactor B and C. Reactor C functioned as a control and sludge backup reactor and was

fed the same influent composition as reactor A. In reactor B three influent composition variations were tested; IVS_1, IVS_2 and IVS_3.

The anaerobic dynamic control strategy was immediately implemented at the start of phase 2. For the entire phase 2, the aerobic and anaerobic control strategy of reactor B and C were operated with the same set-points (CV_1, CV_2, CV_3 and CV_4) as reactor A at the end of phase 1.

In reactor B, the reliability of the anaerobic and aerobic dynamic control strategy during phase 2 was 98.2 %. Automatic activation of the set minimal and maximal anaerobic and aerobic step durations occurred sporadically due to ineffective filling steps.

The anaerobic control strategy was able to adjust the anaerobic step according to the influent COD. The anaerobic MCS profile increased and decreased with an increasing and decreasing influent COD concentration, as was previously reported by Kishida et al. (2008). During IVS_1 a linear correlation between the influent COD and anaerobic step duration was observed with an R^2 of 0.702 and a p-value of < 0.001 ($\alpha = 0.05$), whereas no significant correlation was present during IVS_2 and IVS_3 when the COD/P ratio was varied. The influent PO_4-P and COD/P ratio had no impact on the anaerobic step duration during IVS_2 and IVS_3 (Figure 5 (a) and (d)).

The anaerobic DOC uptake and PO_4-P release efficiencies at grab sample points SPb and SPc (Figure 2) during phase 2 did not change significantly during IVS_1, IVS_2 and IVS_3 (Figure 5(c)). While feeding rapidly varying influent compositions, the anaerobic dynamic control strategy was able to ensure a complete anaerobic DOC uptake.

A significant linear relation between the anaerobic OLR and the influent COD was observed during IVS_1 and IVS_3, with respectively an R^2 of 0.982 and a p-value of < 0.001, and an R^2 of 0.962 and a p-value of < 0.001 (Figure 5 (a) and (b)). Yet the anaerobic control reduced the impact of the influent COD variation on the anaerobic OLR (**Error! Reference source not found.**(d)). Whereas the influent COD variation of 40% would cause a theoretical ORL variation of around 31% in a static anaerobic step, the anaerobic ORL varied around 20%. The influent PO_4-P concentration and the COD/P ratio had no impact on the anaerobic ORL. No linear relation was observed (Figure 5Figure 5(a) and (b)).

The anaerobic P release/COD uptake ratio remained high during phase 2, averaging at 0.42 ± 0.05 during IVS_1 and 0.35 ± 0.09 during IVS_2 and IVS_3. The high anaerobic P release/COD uptake ratio indicates a mature PAO sludge (Oehmen et al. 2006).

The aerobic phase was dynamically controlled depending on the OUR. The influent COD had an impact on the aerobic step duration and the ORL (**Error! Reference source not found.**), but this impact was not significant. The influent PO4-P and COD/P ratio had no impact on the aerobic step duration or the ORL. The main objective of the OUR control was to ensure a complete PO4-P uptake during the aerobic step. As shown in Figure 5(d) the aerobic step periodically showed wide variations. These were caused by the combination of (1) the slow OUR calculation rate (± 20 minutes per value at an endogenous OUR) and (2) the OUR control strategy requirement to have 3 OUR values (SP_{OUR1}) below the endogenous set point. This resulted in elongated aerobic steps.

The rapid influent composition variations had no observed effect on the effluent quality. The control strategy was able to adjust the anaerobic and aerobic step durations to ensure optimal COD and PO_4-P removal. The COD and PO_4-P removal efficiency during the different influent variation strategies remained stable at respectively 95.2 ± 2.7% and 97.7 ± 3.8%. The average COD and PO_4-P effluent concentrations during phase 2 were respectively 58 ± 27 mg/L and 0.53 ± 0.77 mg/L. This is close to the reported effluent PO_4-P concentration by Kishida et al. (2008), lower than < 0.3 mg/L. The conductivity based anaerobic and OUR based aerobic dynamic control strategy was highly effective at achieving low COD and PO_4-P concentrations even during a prolonged period of rapidly varying influent concentrations. Additionally varying COD/P ratios had little effect on the PO_4-P removal efficiency. This increases the potential applications of the control strategy in EBPR systems for the treatment wastewater with a varying composition.

3.2.2 Aerobic Granular Sludge morphology

During phase 2 the AGS in reactor B and C evolved into a hybrid (granular and floccular) sludge. In reactor B the particle distribution (DV50) decreased from 238 µm to 129 µm indicating the formation of hybrid sludge. The same evolution was observed in the control reactor C, the particle distribution (DV50) decreased form 200µm to 135µm. The microscopic images confirmed the evolution into hybrid sludge. Granules remained visible throughout phase 2. The degradation of the AGS in reactor B was not due to applied feeding strategy because a similar AGS degradation was observed in the control reactor C. A possible factor that could have led to the AGS degradation is the reactor

temperature, which was not controlled and thus varied depending on the room temperature..

4.0 Conclusion

The present study investigated a conductivity based anaerobic and OUR based aerobic dynamic control strategy for the removal of PO_4-P in an EBPR AGS SBR which was first fed a constant and then by a rapidly varying wastewater. AGS was successfully formed. The effluent COD and PO_4-P concentrations remained low during the whole study. The anaerobic and aerobic dynamic control strategy elongated and shortened the step durations in line with the influent COD. No aerobic COD leakage was observed.

E-supplementary data of this work can be found in the online version of the paper.

5.0 Acknowledgments

This work was financed by the University of Antwerp through the industrial research fund (IOF) for strategic basic research and was carried out in the research group BioGEM of the Faculty of Applied engineering.

References

1. *APHA, 1998 Standard Methods for the Examination of Water and Wastewater*, 20th edn. American Health Association/American Water Works Association/Water Environment Federation, Washington DC, USA.

2. Caluwé, M., Dobbeleers, T., D'aes, J., Miele, S., Akkermans, V., Daens, D., Geuens, L., Kiekens, F., Blust, R., Dries, J. 2017 Formation of aerobic granular sludge

during the treatment of petrochemical wastewater. *Bioresource Technology* 238, 559-567.

3. de Kreuk, M. K., & van Loosdrecht, M. C. M. 2004 Selection of slow growing organisms as a means for improving aerobic granular sludge stability. *Water Science and Technology* 49 (11–12), 9–17.

4. De Pronk, M., Abbas. B., Al-zuhairy S. H. K., Kraan, R., 2015 Effect and behaviour of different substrates in relation to the formation of aerobic granular sludge. Applied Microbiology and Biotechnology 99, 5257-5268.

5. Dobbeleers, T., Daens, D., Miele, S., D'aes, J., Caluwé, M., Geuens, L., Dries, J. 2017 Performance of aerobic nitrite granules treating an anaerobic pre-treated wastewater originating from the potato industry. Bioresource Technology 226, 211–219.

6. Edgar, R. C. 2013 UPARSE: highly accurate OTU sequences from microbial amplicon reads. *Nature Methods* 10, 996–998.

7. Kishida, N., Tsuneda, S., Sakakibara, Y., Kim, H., Sudo, R. 2008 Real-time control strategy for simultaneous nitrogen and phosphorus removal using aerobic granular sludge. Water science and Technology 58, 445-450.

8. Kozich, J. J., Westcott, S. L., Baxter, N. T., Highlander, S. K., & Schloss, P. D. 2013 Development of a Dual-Index Sequencing Strategy and Curation Pipeline for Analyzing Amplicon Sequence Data on the MiSeq Illumina Sequencing Platform *Applieed and Environmental Microbiology* 79 (17), 5112–5120.

9. Maurer, M., Gujer, W. 1995 Monitoring of microbial phosphate release in batch experiments using electric conductivity. Water Research 29 (11), 2613-2617.

10. Mcilroy, S., Porter, K., Seviour, R. J., & Tillett, D. 2008 Simple and Safe Method for Simultaneous Isolation of Microbial RNA and DNA from Problematic Populations. *Applied and Environmental Microbiology* 74 (21), 6806–6807.

11. Mcilroy, S. J., Saunders, A. M., Albertsen, M., Nierychlo, M., Mcilroy, B., & Hansen, A. A. 2015 MiDAS: the field guide to the microbes of activated sludge. *Database*, 1–8.

12. Oehmen, A., Yuan, Z., Blackall, L., Keller. 2005 Comparison of Acetate and Propionate Uptake by Polyphosphate Accumulating Organisms and Glycogen Accumulating Organisms. Biotechnology and bioengineering 91 (2), 162-168.

13. Oehmen, A., Zeng, RJ., Saunders, AM., Blackall, L., Keller, J., Yuan, ZG. 2006 Anaerobic and Aerobic metabolism of glycogen-accumulating organisms selected with propionate as sole carbon source. *Microbiology-SGM* 152 (9), 2767-2778.

14. Pijuan, M., Guisasola, A., Baeza, J.A., Carrera, J., Casas, C., Lafuente, J. 2005 Aerobic Phosphorus release linked to acetate uptake: influence of PAO intracellular storage compounds.. Bio Engineering Journal 26, 184-190.

15. Sato, H., Matsuo, T., Takashi, M. 1992 Uptake of organic substrate and accumulation of polyhydroxyalkanoates linked with glycolysis of intracellular carbohydrates under anaerobic conditions in the biological excess phosphate removal process. *Water Science Technology* 26 (5), 933-942.

16. Stes, H., Aerts, S., Caluwé, M., Dobbeleers, T.,Wuyts, S., Kiekens, F., D'aes, J., De Langhe, P., Dries, J. 2018 Formation of aerobic granular sludge and the influence of the pH on sludge characteristics in a SBR fed with brewery/bottling plant wastewater. *Water Science Technology* 77 (9), 2253-2264.

17. Vishniac, W., Santer, M. 1957 The thiobacilli. Bacteriol Rev. 21(3), 195-213

18. Weissbrodt, D., Schneiter, G., Furbringer JM., Holliger, C. 2013 Identification of trigger factors selecting for polyphosphate- and glycogen-accumulating organisms in aerobic granular sludge sequencing batch reactors. Water Research 47, 7006-7018.

19. Nereda website: https://www.royalhaskoningdhv.com/en-gb/nereda/nereda-plants, data referenced 10/12/2018

DESCRIPTION FIGURES

Figure 1: (a) Schematic overview of the anaerobic dynamic control strategy, consisting of 3 loops; Loop 1, intermittent logging (every CV_1 seconds) of paired conductivity and timestamp values and building conductivity and timestamp arrays (until the number of pairs in the array reaches a set point value CV_2); Loop 2, intermittent calculation (every CV_1 seconds) of the MCS and comparing the MCS to the maximal MCS set point (until the calculated MCS surpasses the maximal MCS set point CV_3); Loop 3, intermittent calculation (every CV_1 seconds) of the MCS, comparing the MCS to the maximal MCS set point (CV_3) and comparing the counted number of correct MCS to a set point amount to determine anaerobic step termination (until the amount of correct MCS surpasses the maximal amount of the correct MCS set point CV_4). (b) The anaerobic conductivity and MCS profile of the anaerobic dynamic control strategy, (○) MCS, (■) conductivity.

Figure 2: Cycle conductivity profile and grab sample points (SP); SPa, SPb, SPc, SPd and SPe. Highlighted area is the anaerobic step.

Figure 3: Data phase 1; (a) in-situ profiles of reactor A on day 86, (b) OUR and anaerobic and aerobic conductivity MCS profiles on day 86, (c) MLSS, SVI5, SVI30 and DV50 profile of reactor A, (d) Anaerobic time, total OLR and anaerobic OLR profiles of reactor A. The highlighted area in figure (a) and (b) are anaerobic.

Figure 4: qPCR and microbial community composition quantification of *Candidatus Accumulibacter Phosphatis*.

Figure 5: Data phase 2, reactor B; (a) Influent COD and PO_4-P concentration during the different IVSs; (b) Anaerobic and aerobic OLR during the different IVSs; (c) Anaerobic TOC uptake and PO_4-P release efficiency at grab sample point SPb and SPc; (d) Anaerobic and aerobic time during the different IVSs.

569 FIGURE 1

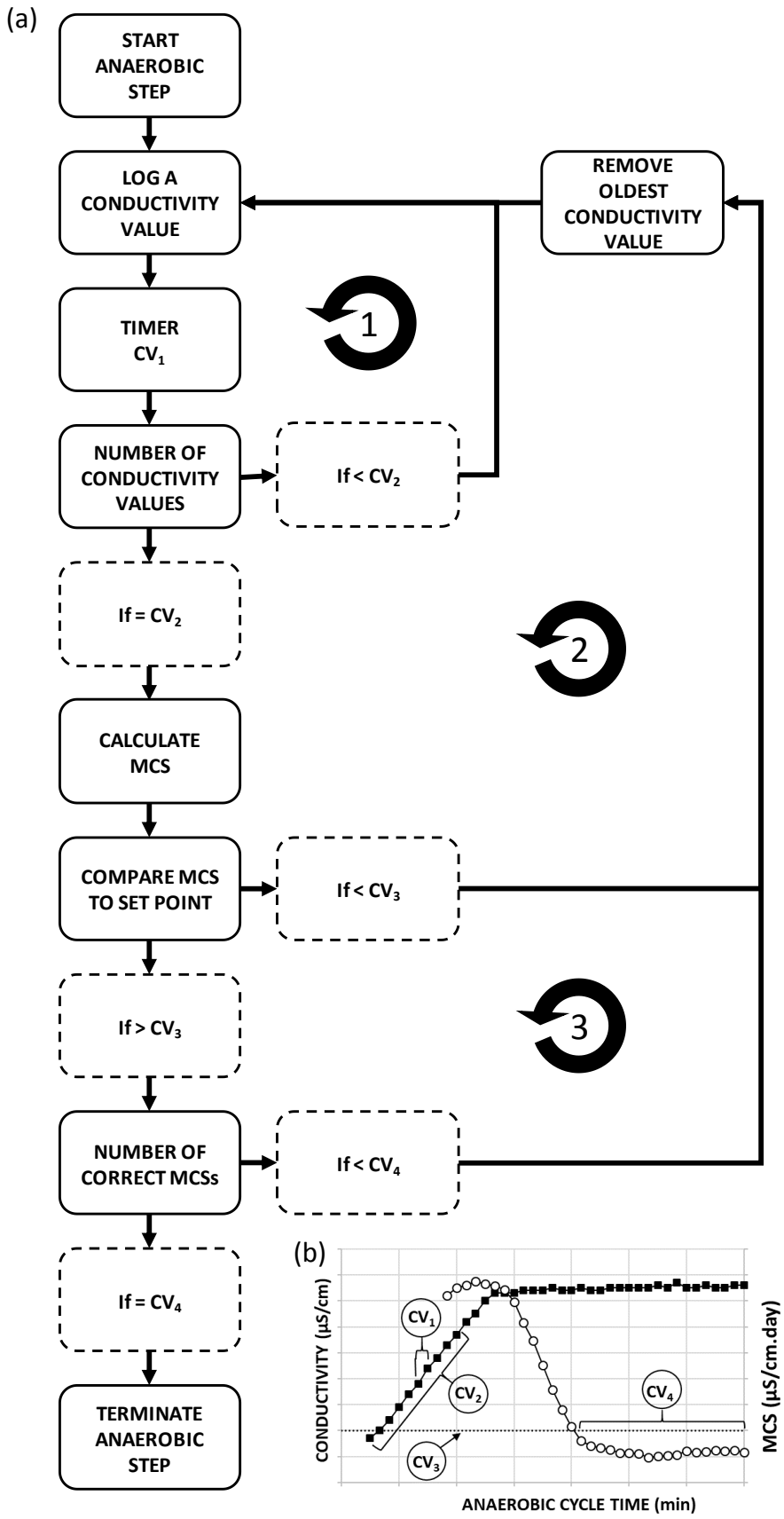

570

FIGURE 2

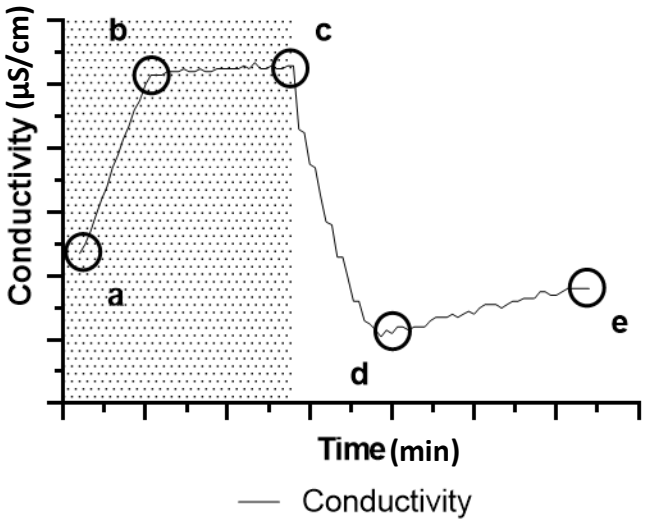

FIGURE 3

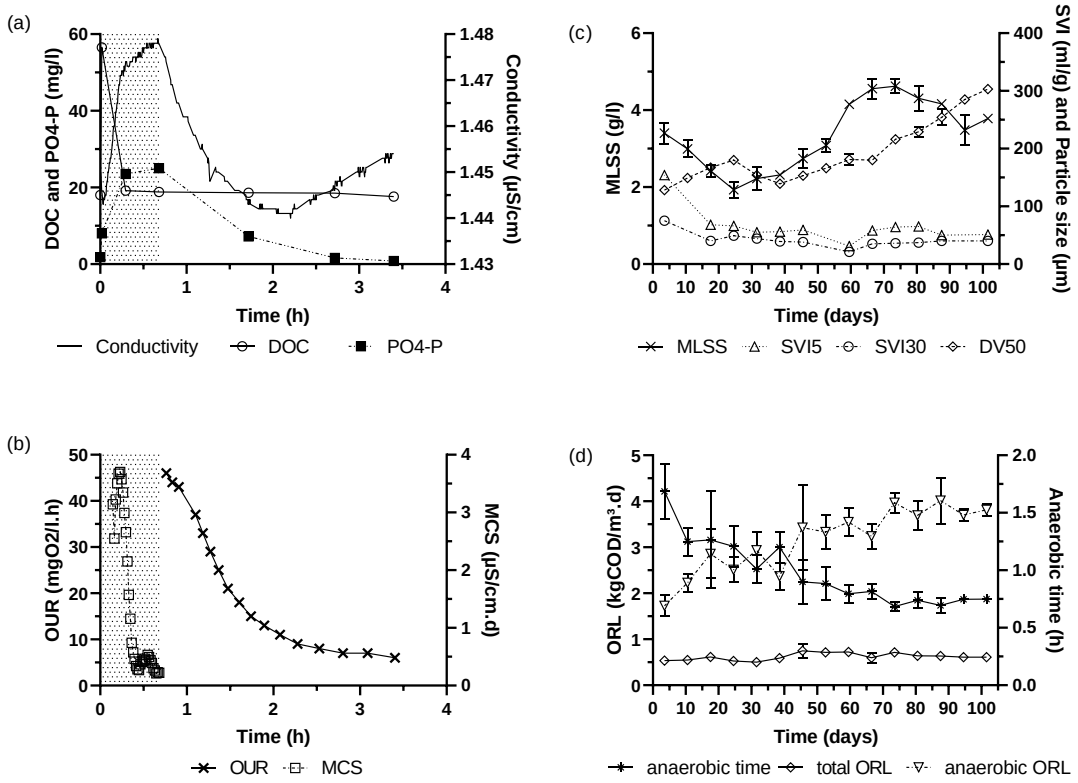

FIGURE 4

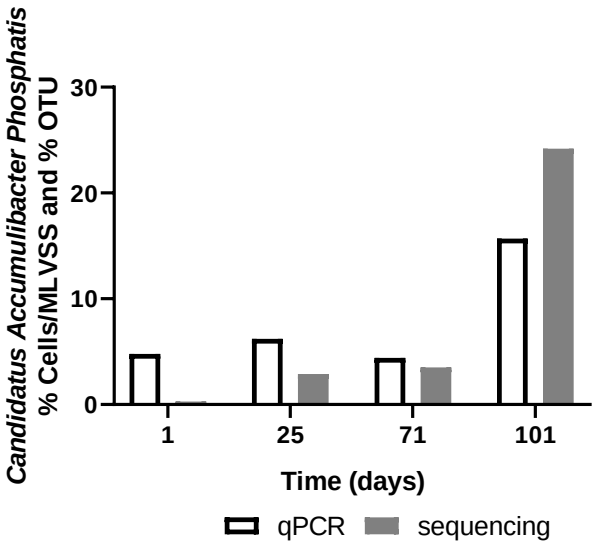

FIGURE 5

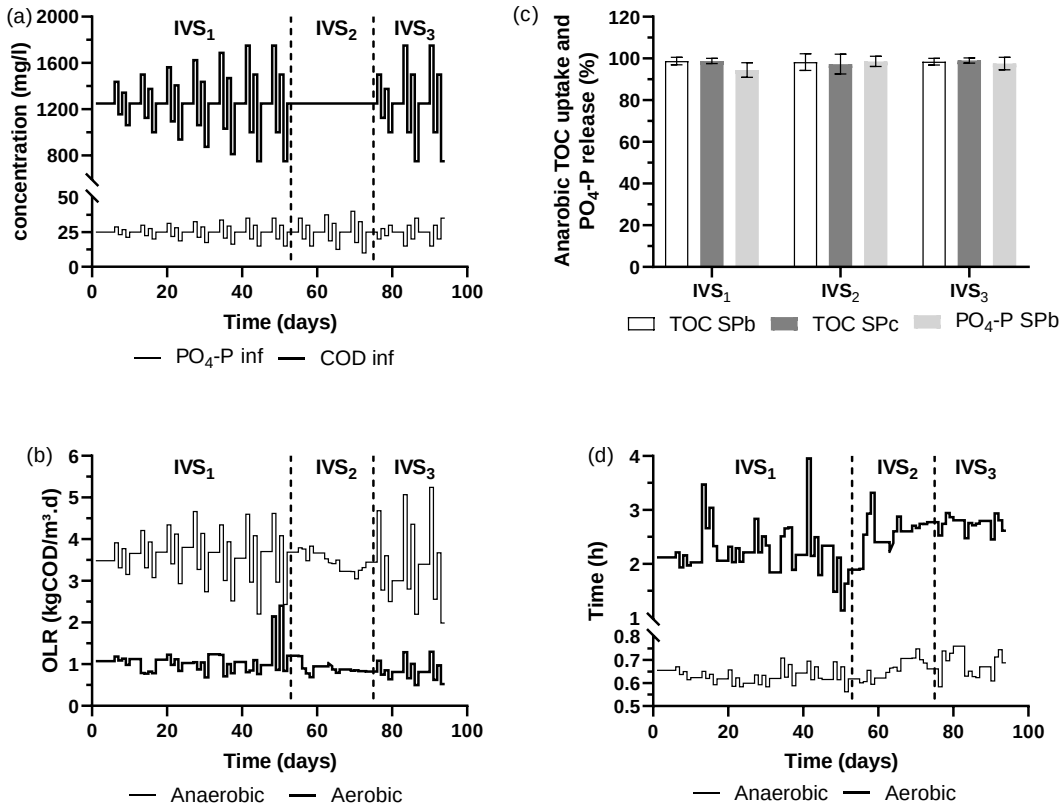

Supplementary Interactive Plot Data (CSV)

Click here to download Supplementary Interactive Plot Data (CSV): SUPPLEMENTARY DATA.docx